Journal of Sound and Vibration 329 (2010) 5273–5288

Contents lists available at ScienceDirect

Journal of Sound and Vibration

journal homepage: www.elsevier.com/locate/jsvi

The directivity of railway noise at different speeds

Xuetao Zhang *

SP Technical Research Institute of Sweden, Box 857, SE-501 15 Boras, Sweden

ARTICLE INFO

Article history:
Received 7 April 2010
Received in revised form
5 July 2010
Accepted 6 July 2010
Handling Editor: L. Huang
Available online 24 July 2010

ABSTRACT

For a sound source, directivity is an important parameter to specify. This parameter also reflects the physical feature of the sound generation mechanism. In this article, studies on the directivity of railway noise, by measurement and by theoretical investigation, are discussed extensively and systematically. The two most important noise types, i.e. rolling noise and aerodynamic noise, are focused on. A model of *perpendicular dipole pair* is proposed to interpret the measurement specified directivity characters of wheel/rail radiation. This model naturally explains why a vibrating railway wheel does not present dipole directivity character and why rail radiation is of different vertical and horizontal directivity characters. Moreover pantograph noise is also found to be of perpendicular dipole components. As for aerodynamic noise around bogies, *scattering* of the air flow is proposed to be the mechanism of the noise generation; this understanding leads to a different directivity description for the noise component. Directivities of other important noise types are discussed as well; their directivities become understood, although lacking of relevant directivity data. In summary, this study provides applicable directivity functions together with a survey of the directivities of all important railway noise types and components. Hopefully, this work will be useful, for railway noise engineering also contribute to understand better railway noise.

1. Introduction

Traffic noise has big impact on our acoustical environment. Estimated, more than 100 millions Europeans are exposed to outdoor equivalent noise levels above 65 dB ($L_{\mathrm{Aeq,\ 24\,h}}$) that scientists and health experts consider being unacceptable [1]. As for railway transportation, although it is considered as the most environmentally friendly means, rail vehicles have been identified as one of the major noise sources, because about 10% of Europeans are exposed to rail noise levels above 55 dB(A) (L_{dn}) [2]. Therefore, a further noise reduction of 10–15 dB(A) in exposure "is necessary across Europe to provide significant improvement in noise exposure levels for the majority of the population affected by railway noise" [3].

Extensive research on railway rolling noise has been carried out since the early 1970s, especially by Remington and his group who setup the preliminary models [4–8] and by Thompson who made major further developments [9]. Thompson's prediction model was implemented into the calculation software Track–Wheel Interaction Noise Software (TWINS) in 1991. The TWINS has proved to be a powerful tool for studying rolling noise and various related noise reduction concepts. Through many following EU-funded research projects on railway noise, this most important noise type of railway noise has become well understood [10]. And, various techniques for reducing railway noise at source have also been developed, such as new brake types, rail and wheel dampers, and acoustical rail grinding scheme [11]. Together with low-noise pantograph

* Tel.: +46 10 516 5021; fax: +46 33 138 381.
E-mail address: xuetao.zhang@sp.se

0022-460X/$ - see front matter © 2010 Elsevier Ltd. All rights reserved.
doi:10.1016/j.jsv.2010.07.003

designs [12–15], it can be concluded that a further noise reduction of 10–15 dB(A) is no longer a technical problem. What we are now looking for is a solution of optimised cost–benefit [11].

Since the early 1990s, when high speed trains became more popular on lines (may be also due to the birth of the TWINS), extensive research on railway aerodynamic noise has been carried out; such research in Europe is mainly within the framework of German–French cooperation [10]. Based on microphone array investigations, together with some wind tunnel studies and numerical simulations, understanding of this noise type has improved [10,16–24]. Briefly, it has been learnt that important aerodynamic noise sources are scattered fluid sound around the bogies, vortex shedding from the pantograph and wake eddies at the train rear, while turbulence noise, radiated from the inter-coach areas, contributes much less.

For a sound source directivity is an important parameter to specify. This parameter also reflects the physical feature of the sound generation mechanism. For example, turbulence sound is of quadrupole directivity, while fluid–structure interaction often produces a sound of dipole character. Therefore, to reach a proper directivity description of a sound source is in fact a process to understand it better. However, this is often not a simple procedure. In railway noise engineering, several noise types of different directivity characters are mixed together, such as wheel and rail radiation, engine and cooling fan noise, scattered fluid sound around bogies and turbulent boundary layer noise along the train side surfaces. Moreover it is a question if the horizontal directivity of a line source can be measured directly. All these factors increase difficulties to achieve a proper directivity description that may explain why modelling the directivities of railway noise sources is much behind modelling their sound powers.

This article intends to make a survey of the directivities of all important railway noise types and components (i.e. rolling noise, aerodynamic noise around pantograph and bogies, turbulent boundary layer noise, traction noise, impact sound, curve squeal, brake noise and bridge vibration noise), also to provide an improved directivity description. In Section 2, the directivity of rolling noise will be discussed first. The basic directivity characteristics of rail and wheel radiation are to be specified based on measurement investigation. A model of *perpendicular dipole pair* will be proposed to interpret the specialty of these directivity characteristics. Further discussed in this section is the horizontal directivity of rolling noise, the speed dependence of it, the effect of high speed motion on it, and the vertical directivity. All (available) directivity studies on rolling noise are to be reflected and some different proposals will have been noticed. As for the aerodynamic noise, its directivity will be discussed in Section 3. Therein proposals of the directivities of aerodynamic component sounds are based on either the measured directivity data (for pantograph noise) or relevant theoretical studies (for turbulent boundary layer noise and scattered fluid sound around bogies). Directivities of other important noise types (i.e. traction noise, impact sound, curve squeal, brake noise and bridge vibration noise) will be discussed as well in Section 4, and concluding remarks will be given in the last section.

2. The directivity of rolling noise

In the past four decades, many measurement studies on the directivity of rolling noise have been carried out [4,25–36]. However, these directivity studies focus on different noise components or operating conditions; the measured directivity data are also greatly dependent on the measurement setups. Understanding of the directivity of rolling noise is not unified; some directivity measurements are even improperly interpreted, due to the reason that directivity pattern of a sound source can be distorted by a number of factors, such as interference between component sound rays, ground absorption and reflection, the shielding and/or reflection and/or diffraction of nearby constructions together with the radiation of the vibrating foundations. Therefore, it will be advantageous to inspect these measurement studies systematically, in order to achieve a directivity description which is not only properly understood, but also useful for engineering applications. In this section, the directivity characteristics of rolling noise will first be specified based on measurement. After that, a model will be proposed to interpret these directivity characteristics. Some studies which proposed different understandings than what will be concluded in this paper will also be discussed, because they may suggest further investigation of the problem. Moreover at high speed, the Doppler factor has significant influence on the horizontal directivity. This effect will be handled in the last sub-section.

2.1. Measurement specified directivities

In 1974, Peters measured the noise profile at 200 m from the track, from a 287 m long passenger train travelling at 144 km/h [25]. By fitting the noise profile data, Peters found that rolling noise was of a dipole-like horizontal directivity. Peters also concluded that wheel radiation dominated in rolling noise, based on the comparison between the measured noise data and the calculated track radiation. Putting these two conclusions together, he proposed that wheel radiation was of dipole directivity character. Unfortunately, this understanding turned out not to be correct. It seems that rail radiation is of dipole directivity character, because around this speed rail radiation dominates [10].

Remington reported his measurements of the directivity of wheel radiation and the vertical directivity of rail radiation [4]. After analysing his data, Remington concluded that these two types of directivities were negligible within 5 dB. Remington did not mention the horizontal directivity of rail radiation, which is probably due to the fact that this quantity cannot be measured directly.

SP's measurements on the directivity of wheel radiation [26,27] support Remington's estimation: wheel radiation in one-third octave bands, at least for those wheels with a curved web, is of a directivity character slightly different from that of a monopole source. Based on the analysis of the wheel radiation data, a more or less frequency independent directivity is proposed [26,27]

$$\Delta L_{\text{wheel}}(\varphi) = 10\lg[0.4 + 0.6\cos(\varphi)], \tag{1}$$

where the angle is relative to the wheel axle and lg is for $\log_{10}$.

Since rail radiation is of dipole directivity in the horizontal direction, which differs much from that given by Eq. (1), relative strength in sound power between rail and wheel radiation plays a role for determining the horizontal directivity of the rolling noise. As was illustrated in [10], for a freight vehicle travelling at 100 km/h on a track equipped with soft rail pads (200 MN/m), the rail radiation contributed about 98.3 dB(A) compared to 94.4 dB(A) by the wheel radiation. However, this example should not be generalised because the relative strength also depends on the train speed. In general, rail radiation contributes more at low speed, while wheel radiation becomes more important at high speed [10].

It then seems acceptable to assume that rail radiation at 150 km/h is about 3 dB stronger than that of the wheels. Since rail radiation is of dipole directivity character in the horizontal direction, while wheel radiation is of the directivity character given by Eq. (1), the horizontal directivity of total rolling noise around this speed is found to be [27,28]

$$10\lg[0.15 + 0.85\cos^2(\varphi)] \tag{2}$$

where the angle is defined as shown in Fig. 1. This function differs slightly from the dipole directivity that Peters concluded for the total rolling noise. (The procedure to achieve Eq. (2) is given by Eq. (3′).)

Moreover to compare prediction models used in Europe, the horizontal directivity functions for rolling noise used in a number of national models are summarized in Table 1 [37]. As can be seen, the directivity function given by Eq. (2) has already been used in Austria, Germany, Switzerland and the Nordic countries. Now, it can be derived. (Note: a directivity description may or may not include a constant, which is the normalisation factor.)

In general, the relative strength in sound power between rail and wheel radiation is given by related track and vehicle transfer functions. Accordingly, a procedure to determine the horizontal directivity of rolling noise in one-third octave

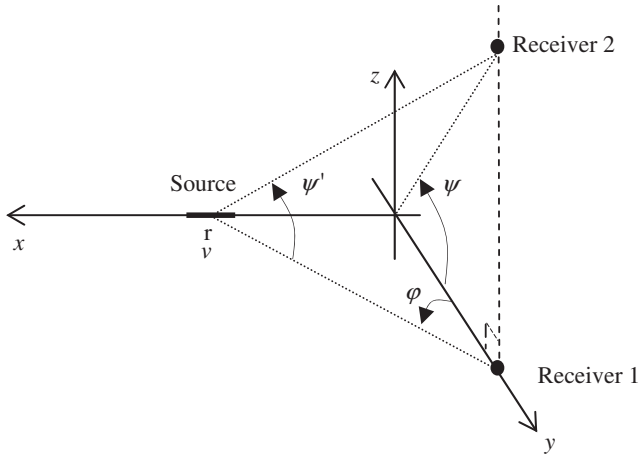

Fig. 1. The definition of angles: φ is a horizontal angle in the x–y plane and relative to the y-axis; ψ is a vertical angle in the y–z plane; ψ' is a vertical angle in a vertical plane containing the receiver and the source (or the centre of the source line).

Table 1
$\cos^2(\varphi)$-like horizontal directivity functions used in Europe [29].

Country	The horizontal directivity function
Austria	$10\lg[0.15+0.85\cos^2(\varphi)]$
Germany	$10\lg[0.22+1.27\cos^2(\varphi)]$ $\cong 10\lg[0.15+0.866\cos^2(\varphi)]+1.66$
Netherlands	$10\lg[\cos^2(\varphi)]$
Switzerland	$10\lg[0.15+0.85\cos^2(\varphi)]+10\lg(2.19)$
Nordic countries	$10\lg[0.15+0.85\cos^2(\varphi)]+2$

bands is proposed [29]:

- The directivity of wheel radiation, D_{wheel}, is given by Eq. (1).
- In the horizontal direction, rail radiation is a dipole source. A practical form of dipole directivity is $D_{\text{dipole}} = 10\lg[0.001 + 0.999\cos^2(\varphi)]$.
- Sleeper vibration is a monopole source.
- The relative strength in sound power between rail/track and wheel radiation is determined by the track and vehicle transfer functions.
- The horizontal directivity of the rolling noise, ΔL_{H}^R, is then given in one-third octave bands by the calculation procedure

$$\Delta L_H^R(\varphi,f) = \begin{cases} D_{\text{wheel}} \oplus \{L_{H,\text{tr}}(f) - L_{H,\text{veh}}(f)\}, & f \le f_{\text{de}} \\ D_{\text{wheel}} \oplus \{D_{\text{dipole}} + L_{H,\text{tr}}(f) - L_{H,\text{veh}}(f)\}, & f > f_{\text{de}} \end{cases} \tag{3}$$

where f_{de} is the de-coupling frequency of the track, $L_{\text{H, veh}}(f)$ the vehicle transfer function, $L_{\text{H, tr}}(f)$ the track transfer function, $\oplus$ energy summation.

For the total sound power of the rolling noise, the horizontal directivity is determined by

$$\Delta L_H^R(\varphi) = D_{\text{wheel}} \oplus \{D_{\text{dipole}} + \Delta L_0\} \tag{3'}$$

where $\Delta L_0 = L_{0,\text{ rail}} - L_{0,\text{ wheel}}$ is the relative strength in sound power between the rail and wheel radiation, with $L_{\text{p, rail}}(\varphi) = L_{0,\text{ rail}} + D_{\text{dipole}}(\varphi)$ and $L_{\text{p, wheel}}(\varphi) = L_{0,\text{ wheel}} + D_{\text{wheel}}(\varphi)$.

The horizontal directivity of total rolling noise at high speed shall differ from that given by Eq. (2) because rail radiation becomes less than the wheel radiation [10]. This shift in dominance directly changes the horizontal directivity. For example, wheel radiation at 350 km/h is estimated to be about 1 dB stronger than the rail radiation; the horizontal directivity of total rolling noise at this speed will then become

$$10\lg[0.23 + 0.35\cos(\varphi) + 0.42\cos^2(\varphi)]. \tag{4}$$

Compared with Eq. (2), this directivity is about 2 dB less directional.

The calculation procedure given by Eq. (3) can be used for any speed, because the transfer functions determine the relative strength in sound power between rail and wheel radiation. These transfer functions do not vary with speed; it is the effective roughness together with train speed that determines the excitation in the frequency domain. For a higher speed, the spectrum of an excitation shifts to higher frequencies, where level differences between track and vehicle transfer functions differ from those at lower frequencies.

SP Acoustics have also measured the vertical directivity of rail vibration noise. The vertical directivity data can be simulated by the function [26,27]

$$\Delta L_{\text{V}}^r(\psi) = 10\lg[0.4 + 0.6\cos^2(\psi)], \tag{5}$$

where ΔL_{V}^r denotes the vertical directivity of rail radiation and ψ is the vertical angle, as shown in Fig. 1. This directivity function differs slightly from that given by Eq. (1).

In practice, the vertical directivity of rolling noise, ΔL_{V}^R, depends not only on the vertical directivities of rail/track and wheel radiation, but also on the shielding effect of the car body which often plays a critical role [27,29]. Since this shielding effect can vary from train to train, then a general formulation for the vertical directivity of rolling noise cannot be expected; a vertical directivity function has to be derived for each train type. Such an example was given in [27,29]: for trains equipped with rectangular-shaped wagons and with their bogies fully exposed, the vertical directivity of rolling noise in one-third octave bands can approximately be formulated as

$$\Delta L_{\text{V}}^R(f,\psi) = 20\lg[1 + f/800]\lg[0.15 + 0.85\cos(\psi)]. \tag{6}$$

The shielding effect of near track construction can also affect the vertical directivity pattern as reported by Chew [30,31], wherein what was investigated is the equivalent vertical directivity, including the shielding by and reflection from the viaduct banks and the radiation from the vibrating viaduct. One other different example of vertical directivity of rolling noise was reported in [32], wherein the vertical directivity data contained significant ground reflection and absorption effects, therefore the results are only of local importance.

2.2. To model the directivity of wheel/rail vibration noise

In an ideal fluid, a small rigid sphere under small amplitude oscillations turns out to be a dipole source [38]. By similarity, it seems that a vibrating rail section can be modelled as a line of dipoles. However, this model can only explain the measured horizontal directivity of dipole character, not the vertical directivity given by Eq. (5) which shows that, in a vertical plane perpendicular to the rail, a vibrating rail section is close to a monopole source. (Here ground effect on the vertical directivity has not been considered.)

As a dipole source is the concern, let us make a close inspection of its directivity character. In Fig. 2, the directivity pattern of a free dipole ($\cos^2\varphi$, with φ being the angle to the dipole axis) is plotted. As can be seen, a free dipole presents

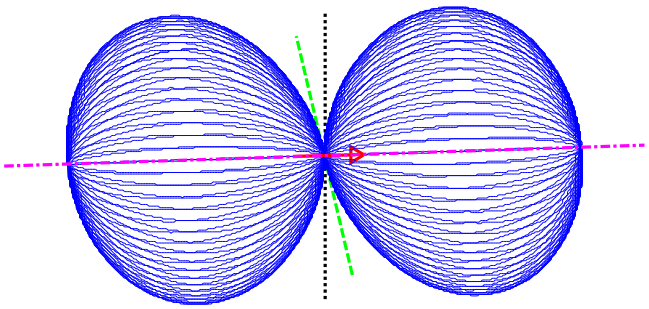

Fig. 2. 3D directivity character of a free dipole.

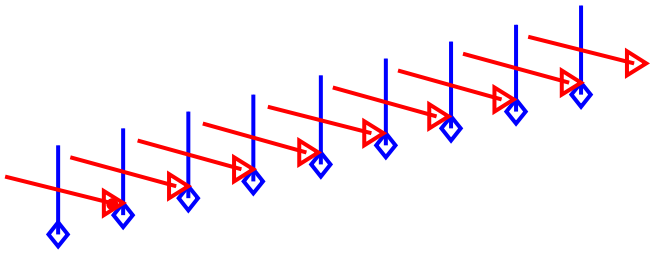

Fig. 3. A straight line of perpendicular dipole pairs used to model the directivity of rail vibration noise.

dipole directivity character in a plane containing the dipole axis. However, in a plane perpendicular to the dipole axis, the free dipole presents monopole directivity character! This fact suggests that, when considering directivity effect of a dipole source, the orientation of its axis needs to be specified.

With this understanding, a trial model of a straight line of perpendicular dipole pairs is made for simulating the directivity of rail vibration noise. As is shown in Fig. 3, a straight line of dipoles with vertical orientation simulates rail head and foot vibration, while a straight line of dipoles with lateral orientation simulates rail web vibration. And, the latter is assumed being about 4 dB stronger in sound power than the former.

In a horizontal plane located about half the rail height, the line of dipoles with vertical orientation presents monopole directivity character (and is of negligible sound power), while the line of dipoles with lateral orientation presents dipole directivity character. Combined horizontal directivity of the dipole pair is of dipole character. However, in a vertical plane perpendicular to the rail, they both present dipole directivity character. Thus, combined vertical directivity of the dipole pair depends on the relative strength in their sound powers. If they were the same in sound power, combined vertical directivity would be of monopole character because $\cos^2(\psi)+\cos^2(\psi+\pi/2)=1$. Since the line of dipoles with lateral orientation is assumed being 4 dB stronger in sound power, combined vertical directivity is then determined by the following procedure

$$L_{p,\mathrm{dipole1}} = L_0 + 10\lg[0.001 + 0.009\cos^2(\psi+\pi/2)], \tag{7}$$

$$L_{p,\mathrm{dipole2}} = L_0 + 10\lg[0.001 + 0.009\cos^2(\psi)] + 4, \tag{8}$$

$$L_{p,\mathrm{combined}} = 10\lg(10^{L_{p,\mathrm{dipole1}}/10} + 10^{L_{p,\mathrm{dipole2}}/10}). \tag{9}$$

where L_0 is a constant; dipole 1 is of vertical orientation and dipole 2 of lateral orientation. The numerical result shown in Fig. 4 indicates that Eqs. (7)–(9) produce a vertical directivity identical to the one given by Eq. (5). Thus, it has been proved that the model of a straight line of perpendicular dipole pairs can properly simulate both the vertical and horizontal directivity characteristics of the rail vibration noise.

Next, the directivity of wheel vibration noise is to be modelled in a similar way. A circular line of dipoles with radial orientation simulates wheel tread vibration and a circular line of dipoles with an axial orientation simulates wheel web vibration, as shown in Fig. 5. Again, the latter is assumed being about 4 dB stronger in sound power than the former. As has already been learnt, in a plane which contains the wheel axle, the combined directivity should be determined by Eqs. (7)–(9) that will result in a directivity pattern the same as that given by Eq. (5). This directivity is slightly different from the measured one simulated by Eq. (1). However, the difference between these two directivity functions is quite small and can be ignored. (In fact, it has been tried out that a combined directivity closer to Eq. (1) can be achieved if taking a level difference of 3.5 dB and an orientation difference of 80° between the components of the dipole pair. However, this small "correction" is not used here considering that the main concept, rather than the details, should be focused on.)

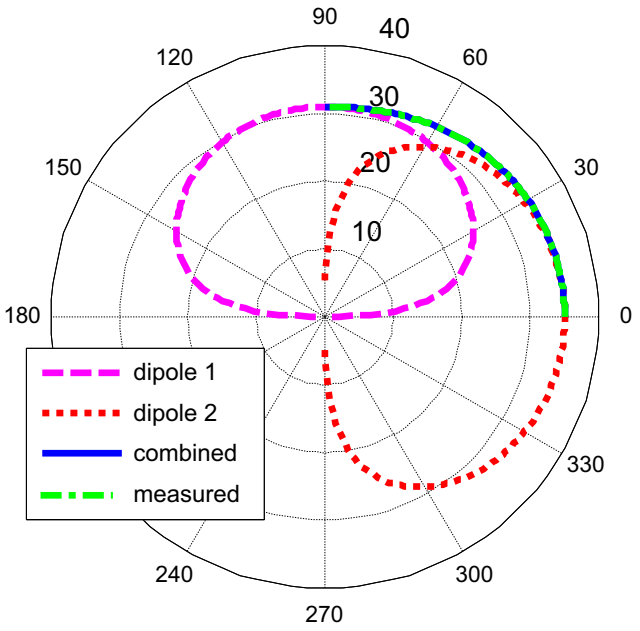

Fig. 4. Comparison between measured vertical directivity of rail radiation and the one predicted by the model of perpendicular dipole pair, "combined," where the directivities of dipole 1, dipole 2, and "combined" are given by Eqs. (7)–(9), respectively.

These good results reflect the value of the model: it is promising for understanding the wheel/rail vibration noise. This model naturally explains why a vibrating wheel does not present dipole directivity character and why rail radiation is of different vertical and horizontal directivity characters. Moreover, it also indicates that, for a dipole source, the orientation of its axis needs to be specified when considering its directivity effect. Especially, if more than one dipole is concerned, a special disposition of the dipoles together with a selection of difference in their sound powers can result in a directivity pattern from that of monopole character to that of dipole one.

It is easy to construct the vertical directivity of wheel–rail vibration noise, because the directivity of wheel radiation given by Eq. (1) differs only slightly from the vertical directivity of rail radiation given by Eq. (5). One can use either of them to describe the vertical directivity of the wheel–rail vibration noise.

Eq. (3) provides a procedure to construct the horizontal directivity of the wheel–rail vibration noise, which can be derived in the following. Taking the description of roughness (L_r) and transfer function ($L_{H,\,tr}$ for rail/track and $L_{H,\,veh}$ for wheel/vehicle) [39], sound pressure levels of wheel/rail vibration noise can be written as

$$L_{p,\mathrm{rail}} = L_{H,\mathrm{tr}} + L_r + L_c + D_{\mathrm{dipole}}, \tag{10}$$

$$L_{p,\mathrm{wheel}} = L_{H,\mathrm{veh}} + L_r + L_c + D_{\mathrm{wheel}}, \tag{11}$$

$$\begin{aligned} L_{p,\mathrm{combined}} &= 10\lg\left(10^{L_{p,\mathrm{rail}}/10} + 10^{L_{p,\mathrm{wheel}}/10}\right) \\ &= L_{H,\mathrm{veh}} + L_r + L_c + 10\lg\left(10^{(D_{\mathrm{dipole}} + L_{H,\mathrm{tr}} - L_{H,\mathrm{veh}})/10} + 10^{D_{\mathrm{wheel}}/10}\right) \end{aligned} \tag{12}$$

where $L_c = 10\lg(N_{\mathrm{axle}}/L_{\mathrm{wagon}})$ is a correction term for the number of axles per wagon and the wagon length. The last term in the second equation in Eq. (12) gives the second equation in Eq. (3). The first equation in Eq. (3) is due to the fact that sleeper vibration noise is a monopole source.

2.3. Some arguments

Wolde and Ruiten [33] reported that their extensive measurement investigation on the wheel/rail vibration noise supported Remington's results in many aspects, except the directivity of wheel radiation. Based on their data, they concluded that a uniform directivity model could be accepted only within $\pm 30^\circ$ from the wheel axle; otherwise it was too simple. Since they did not describe their data of wheel directivity, it is impossible to make a further discussion.

It is interesting to look at the data of wheel directivity presented in [34]. Briefly, for wheels with a straight web, radial modes are of monopole character and axial modes are of dipole character. However, results for wheels with a curved web "resembled the radial mode results …, since the predominantly axial modes also contain radial motion". These wheels, of a diameter of 920 mm, were excited at several natural frequencies and the directivity data were measured around a semi-circular frame of radius 1.5 m, which is centred at the wheel centre.

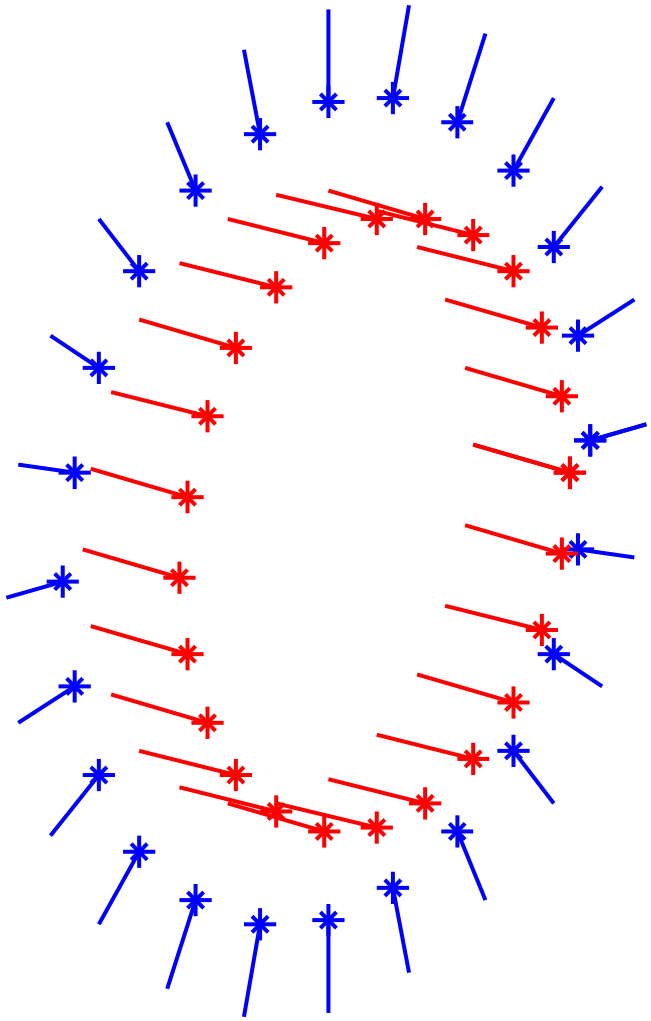

Fig. 5. A circular line of perpendicular dipole pairs used to model the directivity of wheel vibration noise.

Since the directivity data presented in [34] contain significant interference effects, carefulness should be paid and some further investigation may need to be considered before drawing a conclusion on the directivity for wheels with a *straight* web. As was recommended in [29], a larger measurement radius, about 4–6 times the wheel diameter, shall be used. Moreover, for such wheels, directivity data in one-third octave bands shall also be investigated, because in engineering a sound source is often described in the one-third octave bands.

In [33], it was proposed that rail vibration in horizontal direction is a dipole source, because rail vibration decays along the two sides. However, decaying sound power levels can be assigned to a line of incoherent monopole sources to simulate rail decay. Thus, in itself, a decay feature does not necessarily require dipole directivity character.

An investigation on sound radiation from waves in rails using two-dimensional boundary element method was reported [35]. About the horizontal directivity of rail radiation, complicated results were presented in the paper. Roughly speaking, for a track with soft pads, all wave types, except lateral bending wave, radiate the same or more sound power in rail lateral direction than a dipole source does. For lateral bending wave in rails, it radiates like a dipole source below about 80 Hz; above 80 Hz it gradually shifts to a monopole source until 160 Hz. It will then continuously shift to radiate more power in rail direction between 160 and 200 Hz and, above 200 Hz, it begins to shift back to a monopole source until 300 Hz. (Beyond 300 Hz, no result was given.) A coherent line source of the same power was used for simulating rail vibration.

In [36], the authors stated that "below 1 kHz the radiation ratio of a rail resembles that of a line dipole, while above 1 kHz it is close to unity. … the results presented here are found not to differ greatly whether monopoles or dipoles are used. Monopoles are therefore used for simplicity". (According to the description in [35] (although not explicit), the radiation ratio seems to mean the ratio of the sound power radiated into the vertical plane (perpendicular to the rail) to the overall sound power radiated from the rail.) It seems that the authors proposed: (1) a line of coherent monopoles can simulate a dipole source; (2) a line of coherent monopoles are equivalent to a line of coherent dipoles. However, these two statements are questionable. It is understood that numerical results depend on many factors. Under certain conditions,

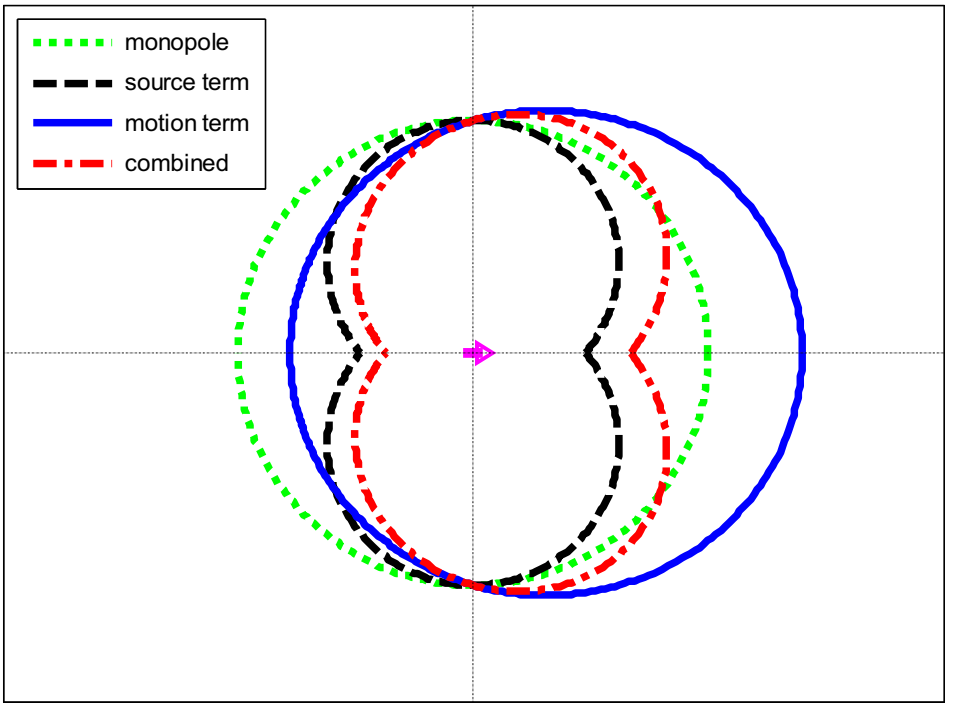

Fig. 6. The horizontal directivity of rolling noise at 350 km/h. The "source term" is given by Eq. (4), wherein wheel radiation has been assumed 1 dB stronger than rail radiation. The "combined" is given by Eq. (14) and "motion term" is the second term on the right hand side of Eq. (14).

a line of monopoles may give the same results as that of a line of dipoles; while, these two source types are in general not the same. For example, their directivity effects are not much different for a close receiver, while distinct for a distant observer [29]. Therefore, a proper directivity description should not only be based on certain measurements or/and numerical calculations, but also have the physics behind the phenomenon respected.

2.4. The Doppler factor

For a fast moving sound source, the Doppler factor has to be considered. This factor is described as [40]

$$[1-M\cos(\theta)]^{-2(n+1)} = [1-M\sin(\varphi)]^{-2(n+1)}, \tag{13}$$

where $M=u/c$ is the Mach number, angle $\theta=\pi/2-\varphi$ is relative to the track, while φ relative to the lateral direction of the track. $n=0$ is for a moving point monopole source, $n=1$ for a moving volume monopole or force dipole source, $n=2$ for a moving quadrupole source, and so on.

Thus, at high speed, the combined horizontal directivity of rolling noise consists of two components

$$\Delta L^R_{H,\text{combined}}(\varphi,f) = \Delta L^R_{\text{H}}(\varphi,f) - 20\lg[1-M\sin(\varphi)], \tag{14}$$

where $\Delta L^R_{\text{H}}(\varphi,f)$ is determined by Eq. (3). For making the following discussions easier, the first term in Eq. (14), $\Delta L^R_{\text{H}}(\varphi,f)$, is named as *source term*, because it depends on the directivity character of a sound source. Naturally, the second term, the Doppler factor, is named as *motion term*.

As an example, let us consider the horizontal directivity of rolling noise at 350 km/h. The source term, $\Delta L^R_{\text{H}}(\varphi)$, is given by Eq. (4) if the wheel radiation around this speed is about 1 dB stronger than that of the rail. The combined horizontal directivity together with those of its components are depicted in Fig. 6. As can be seen, both source and motion terms are important for a directivity description of rolling noise at high speed.

3. The directivity of aerodynamic noise

Research on railway aerodynamic noise is much behind that on the rolling noise. As for measurement, the data of aerodynamic noise around bogies is obtained by subtracting rolling noise contribution from the measured total, where rolling noise is calculated using the TWINS together with the consideration of the Doppler factor and directivity. Obviously, the accuracy of the directivity data of aerodynamic noise around bogies obtained in this way is lower than that of the rolling noise. On the other hand, as for model simulation, there are only simple case studies simulating pantograph noise or fluid–cavity-interaction noise [14,21–24]. For the dominant noise component around bogies, where scattered fluid sound

is the concern, there is no proper calculation method available presently [20]; therefore, only qualitative studies can be made.

In this section, first, it will be discussed what have been learnt about the directivity of railway aerodynamic noise. Next, directivities of different components of aerodynamic sound will be either described or proposed. The discussion will also lead to a proposal for separating aerodynamic noise around bogies from the rolling noise.

3.1. What have been learnt about the directivity of railway aerodynamic noise

3.1.1. The Harmonoise proposal for the directivity of aerodynamic noise

During the European project Harmonoise, a preliminary directivity estimation for various aerodynamic noise sources was proposed [17], as summarized in the following: (1) one set of directivity data of pantograph noise were provided in tabular values, which show dipole directivity character in the horizontal direction (will be proved later) and about 4 dB higher level in the vertical direction than in the lateral direction; (2) inter-coach noise is less directional than aerodynamic sound around bogies; (3) due to a lack of information about their directivity, all sub-sources, except pantograph noise were assigned the same directivity which is given by

$$5\ln[\sin(\varphi+\pi/2)]. \tag{15}$$

3.1.2. The directivity of pantograph noise

The directivity of pantograph noise has been measured at 280 km/h [17]. The directivity data were given in tabular values in the angle range of [0°, 180°]. Although the measurement specification is not provided, it can be checked out by inspecting the effect of the Doppler factor that the downstream direction is at 0°. Since horizontal angles used in this paper differ from those used in [17] by 90°, the transformed angle range shall be used which can easily be found to be [0°,180°] $-90°=[-90°,90°]$.

By trial and error, it is found that the horizontal directivity of the measured pantograph noise can be simulated by the following equations

$$\Delta L_{\text{pantograph}} = 10\lg[0.006+(1-0.006)\cos^2(\varphi)], \tag{16}$$

$$\Delta L_{\text{Doppler}} = -40\lg[1-M\sin(\varphi)], \quad M=u/c, \tag{17}$$

$$\Delta L_{\text{combined}} = \Delta L_{\text{pantograph}} + \Delta L_{\text{Doppler}}. \tag{18}$$

The numerical result of this simulation procedure is shown in Fig. 7(a). The source term, given by Eq. (16), confirms that the pantograph noise is of dipole directivity character in the horizontal direction. And, in a vertical plane perpendicular to

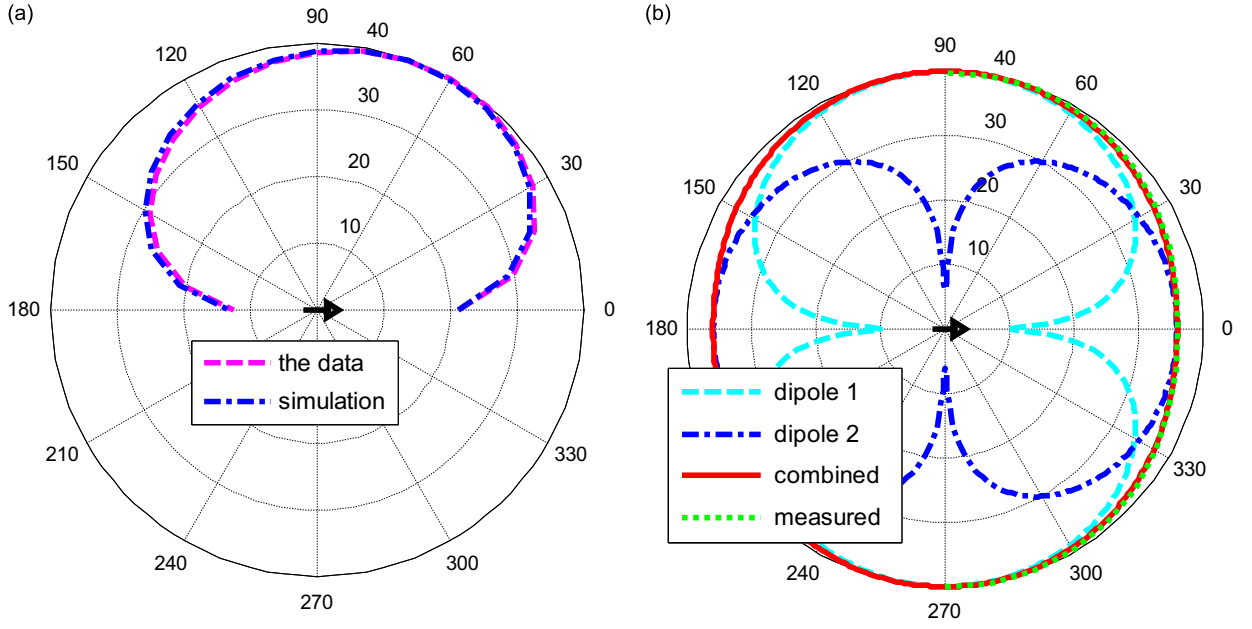

Fig. 7. (a) The measured horizontal directivity of pantograph noise [17] compared with the simulation directivity function formulated by Eqs. (16)–(18). (b) The measured vertical directivity of pantograph noise compared with the simulation of perpendicular dipole pair of which the dipole with lateral orientation is 4 dB weaker.

the train, the directivity data given in [17] indicate about 4 dB lower level at angle position of 90° compared with that at 0° or 180°. Although it was not specified in [17], angle position of 90° should be for level direction. This vertical directivity together with the horizontal directivity can easily be interpreted by the model of perpendicular dipole pair as shown in Fig. 7(b): in vertical direction, vortex-induced vibration (VIV) can under certain conditions cause an Aeolian sound [15]. An Aeolian sound is a dipole source [40], with an orientation transverse to the flow and the sliding bow. Thus, this VIV sound is a dipole source of vertical orientation and a sound power of about 4 dB stronger than the second dipole source, which has its dipole axis in the lateral normal direction of the train. In a horizontal plane, the VIV sound, which presents dipole directivity character in a vertical plane, presents monopole directivity, while the second dipole source presents dipole directivity.

It is not sure to the author what mechanism generates this second dipole source. It could be the interaction between the air flow and the two end parts of the sliding bow of a pantograph that induces a lateral vibration, compared with the lift force on the middle part of the sliding bow, where the (vertical component of the total) VIV sound is induced. (The second dipole source could be the lateral component of the total VIV sound.)

3.1.3. The directivity of turbulent boundary layer noise

The directivity of turbulent boundary layer noise has been worked out by Tam [41]. Tam started with the wave equation of the problem, adopted an empirical model of wall pressure cross-correlation function proposed by Maestrello [42,43], and then solved the problem and obtained the intensity, spectrum, and directivity of the turbulent boundary layer noise (Tam's turbulent boundary layer is of an infinite extent; or, physically, the edge effect is negligible). Tam obtained the total directivity function (named as *broadband directivity* in his paper, which depends only on the Mach number) and the one in frequency (in fact in Strouhal number). These directivity functions have the following characteristics:

- On a cross section perpendicular to the flow, the directivity is symmetric and slightly less directional than a free dipole.
- On a cross section parallel to the flow, the directivity at small Strouhal numbers is almost the same as the counterpart on a cross section perpendicular to the flow. While, the directivity at larger Strouhal numbers is not only less directional than a free dipole but also *tilts in the downstream direction*. Moreover for the total directivity, it *tilts in the downstream direction* by an angle slightly greater than $\tan^{-1} M$, where M is the Mach number of the flow. (The effect of mean flow has not been included.)

Tam explained these characteristics as: (1) being (slightly) less directional than a free dipole because of the *severe geometrical constraint*; (2) tilting in the downstream direction because of the *convection*.

Tam's directivity function in frequency (or, stringently, in Strouhal number) contains the modified Bessel function of order zero and a summation over the parameter space. The total directivity contains a further integration over Strouhal number. Tam provided some examples of the directivity functions at several typical values of Strouhal number and Mach number to show the directivity characteristics mentioned above. However, the directivity function, either of frequency component or of the total, is too complicated to be directly used in engineering, or to be suitable for comparisons. Therefore, a set of formulae have been worked out to simulate the total directivity in a plane containing the flow

$$\Delta L^P(\varphi) = 10\lg[0.001 + 0.75\cos(\varphi) + (0.25-0.001)\cos^2(\varphi)], \tag{19}$$

$$\Delta L_0(\varphi) = \lg\left[1+\sin\left(\varphi\frac{3\tan^{-1}M}{\pi}\right)\right], \tag{20}$$

$$\Delta L_{\mathrm{H}}^{Turbulent}(\varphi) = \begin{cases} \Delta L^P + 10\Delta L_0, & \text{if } \varphi < 0 \\ \Delta L^P + 20\Delta L_0, & \text{if } \varphi \geq 0 \end{cases}, \tag{21}$$

where $\varphi = -\pi/2$ is for the downstream direction. Eq. (19) simulates the directivity on a cross section perpendicular to the flow. This directivity is shown in Fig. 8(a) for M=0.7 and in Fig. 8(b) for M=0.29 (corresponding to 350 km/h). The angle used in Fig. 8 has been transformed by adding 90°, therefore angle position of 90° is for the direction perpendicular to the flow and angle position of 0° for the downstream direction.

Fig. 8(a) also shows that the directivity function proposed for aerodynamic noise by Charbonnel [17], given by Eq. (15), is exactly the same as that given by Eq. (19). Thus, the Harmonoise proposed directivity for aerodynamic noise (except pantograph noise) is in fact that for the turbulent boundary layer (of infinite extent) noise, which is slightly less directional than a free dipole. (It will be shown later why this proposal does not seem to be correct.)

3.1.4. The directivity of scattered fluid sound

Let us consider a plane, time-harmonic sound wave $p_{\mathrm{I}} = p_0 e^{i\kappa_0 x_1}$ incident on an acoustically compact spherical inclusion of radius R. According to the Rayleigh scattering, if the sphere is fixed and rigid, the scattered fluid sound will be [40]

$$p_{\mathrm{S}} \approx \frac{-p_0(\kappa_0 R)^2}{3|\vec{x}|}\left(1-\frac{3}{2}\cos\theta\right)e^{i\kappa_0|\vec{x}|}, \quad |\vec{x}| \to \infty. \tag{22}$$

where θ is the angle between the radiation direction and the incident wave.

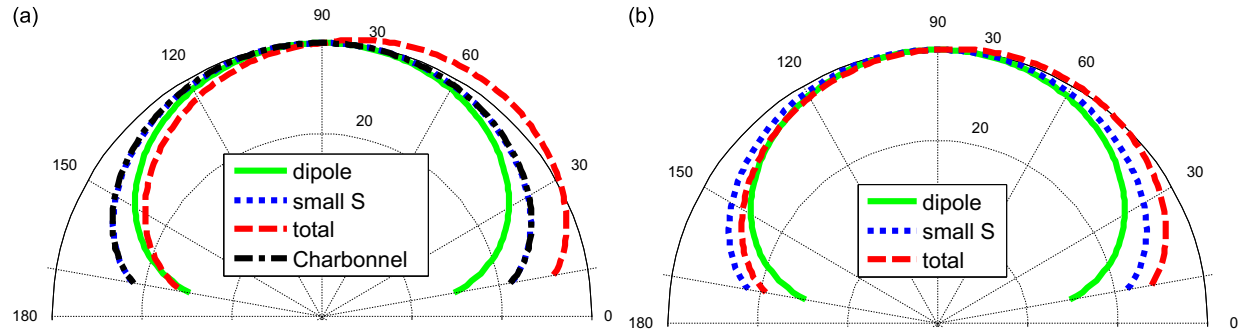

Fig. 8. Comparison between various directivity functions: "small S" denotes the directivity for small Strouhal number components given by Eq. (19); "total" is the tilted total directivity of turbulent boundary layer noise simulated by Eqs. (19)–(21). (a) M=0.7; "Charbonnel" denotes the directivity proposed by Charbonnel, given by Eq. (15), which overlaps the directivity of "small S"; (b) M=0.29 (V=350 km/h). 0 degree is for the downstream direction.

For a flow over a *rough wall*, whose characteristic roughness height R is much smaller than the boundary layer thickness δ, it has been concluded that, when $\omega R/v_* > 5$, where v_* is the friction velocity, the dominant mechanism of noise generation is *scattering* [40]. An empirical spectrum for the whole frequency range is approximately given by

$$\frac{\Phi_R(\vec{x},\omega)}{\rho_0^2 v_*^3 \delta} \approx \tau_0 \frac{A\cos^2\theta}{|\vec{x}|^2} \frac{R}{\delta} \frac{v_*^2}{c_0^2} \frac{(\omega R/v_*)^3}{[1+\beta(\omega R/v_*)^2]^\gamma}, \tag{23}$$

where θ is the angle between the radiation direction and the incident wave. τ_0, β and γ are empirical constants; c_0 is the speed of sound and A the area of the rough wall. β=0.0025 and γ=5.5 are tentative values. Moreover, for low roughness density, there will be $\tau_0 \approx (v_*/U_C)^2(\alpha/\pi)$, where $\alpha = N\pi R^2$ and N is the number of rough elements per area. $U_C \approx 0.5U - 0.7U$ is the translational speed of the principal boundary layer eddies and U the velocity of the free stream [40].

3.2. The directivity of aerodynamic noise

Based on the measured directivity data of the pantograph noise [17], the horizontal directivity can be simulated by Eqs. (16)–(18). The vertical directivity can be interpreted by the model of perpendicular dipole pair: the (vertical component of) VIV sound is a dipole source with vertical orientation and about 4 dB stronger in sound power than the second dipole which is (probably, the lateral component of the VIV sound and) of the lateral orientation.

Turbulent boundary layer noise is a sound source of nearly dipole character, as has been proved by Tam [41]. The dipole axis is in the normal direction of the boundary layer, if a negligible tilt is concerned. The exact directivity is given by Eqs. (19)–(21), where Eq. (19) is equivalent to Eq. (15). However, for railway applications, this noise source is less important [16–18].

Based on his theoretical investigation, Tam also indicated that convection effect causes the horizontal directivity of turbulent boundary layer noise tilting in the downstream direction. However, the measured horizontal directivity of the pantograph noise is not of this kind of tilt. This discrepancy between the theoretical investigation and measurement may be due to the difference between the two situations: in Tam's situation, the aerodynamic sources flow away from the receiver, while in the situation of train pass-bys pantograph induced aerodynamic sources are of no important motion relative to a wayside receiver. Thus, since train pass bys are relevant, this convection effect will not be considered in the directivity description.

Aerodynamic sound generated around bogie regions is the most important component of railway aerodynamic noise; its generation mechanism was assumed to be flow separation and recirculation [16,17]. However, it seems that *scattering* of the air flow is the dominant mechanism for the phenomenon. As has been described in Section 3.1.4, this scattered fluid sound has its dipole axis in the downstream direction.

Thus, aerodynamic noise generated along a side surface of a train due to fluid–structure interaction can again be modelled as a line of perpendicular dipole pairs: boundary layer noise has its dipole axis in the direction of the normal to the wall and scattered fluid sound has its dipole axis in the the downstream direction. Although the latter predominates, boundary layer noise may prevail in the normal direction, due to the directivity characters of the two dipole components.

The combined directivity of this perpendicular dipole pair could, by a calculation procedure similar to that given by Eqs. (7)–(9), easily be constructed if the relative strength in sound power between the two dipole components were known. However, this information is not available presently. Thus, an estimation is made. If we assume that the scattered fluid sound is 15 dB stronger in sound power than turbulent boundary layer noise, the combined directivity will be

$$\Delta L_H^A(\varphi) = 10\lg[C_1 + (1-C_1)\cos^2(\pi/2-\varphi)], \quad C_1 = 0.03, \tag{24}$$

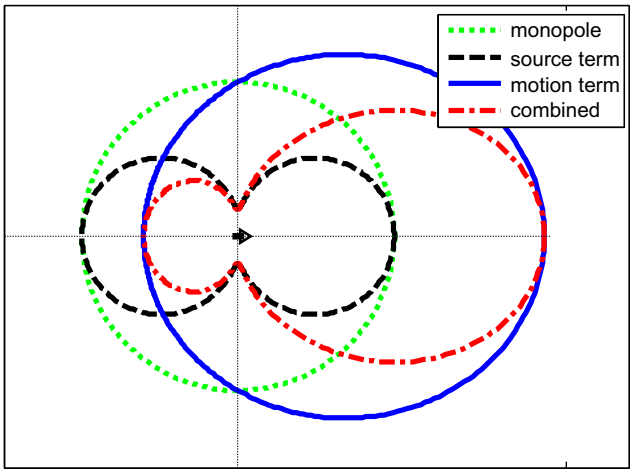

Fig. 9. The horizontal directivity of scattered fluid sound and boundary layer noise at 350 km/h. The "source term" is given by Eq. (24). The "combined" is given by Eq. (25) and "motion term" is the second term on the right hand side of Eq. (25).

where the horizontal angle, φ, is relative to the lateral normal, as shown in Fig. 1. This directivity function indicates that, for the combined horizontal directivity of the perpendicular dipole pair, boundary layer noise is equivalent to a small monopole component described by C_1. Moreover if the difference in sound power between the two dipole components is 10 or 20 dB, there will be $C_1=0.1$ or 0.01, respectively.

Since all important aerodynamic noise sources are of dipole character, the Doppler factor for aerodynamic noise is given by Eq. (13) with $n=1$. The combined horizontal directivity of scattered fluid sound, for example, is then determined by

$$\Delta L^A_{H,\mathrm{combined}}(\varphi)=\Delta L^A_{\mathrm{H}}(\varphi)-40\lg[1-M\sin(\varphi)], \tag{25}$$

where the source term, $\Delta L^A_{\mathrm{H}}(\varphi)$, is given by Eq. (24) if boundary layer noise is 15 dB weaker. This combined horizontal directivity of scattered fluid sound at 350 km/h is depicted in Fig. 9. As can be seen, most sound power of it is emitted in the forward direction, due to the effect of the Doppler factor.

This directivity character of scattered fluid sound also suggests a possibility to separate aerodynamic noise around bogies from the rolling noise. Let us consider a train speed of about 350 km/h, at which aerodynamic noise and rolling noise are likely comparable [16]. Let us also assume that, for some wagons which are located enough far away from a pantograph, pantograph noise is less important or can be separated. Thus, rolling noise dominates in the lateral normal direction, while scattered fluid sound dominates in the direction of motion, due to their directivity characters. To record railway noise at or near these two special angle positions will probably achieve the separation of the two noise components.

4. Directivities of other important noise types

Important sources of railway noise other than rolling noise and aerodynamic noise are traction noise, impact sound, curve squeal, brake noise and bridge vibration noise [10].

In history, traction noise could be important even up to 200 km/h [44]; today, it is a dominant noise type at low speed. For example, SP has measured the noise sound power of a diesel-electric locomotive of GB T66 type. It is found that, when the locomotive runs at its full traction effort, the traction noise cannot beat the rolling noise at 40 km/h [45]. Obviously, modern traction units are much quieter than old ones. Moreover, for modern traction units, the dominant traction noise sources are cooling fans and traction engine/motor(s). This understanding has been confirmed by a recent investigation on the noise emission [46].

As for engine noise, considerable variations in sound power between engines of the same combustion system are "still not fully understood in spite of the large amount of theoretical and analytical work that has been carried out" [44]. As for fan noise, the mounting connection or/and housing condition can have significant influence on the noise generation [44,47]. This wide variety in sound power impedes a universal description in modelling traction noise; neither the sound power nor the directivity can be formulated in a general manner.

Based on measurement, the monopole directivity is estimated for diesel-electric locomotive noise due to the typical high peak around 80–125 Hz in its sound power [44,45]. For cooling fan noise, the type of a fan and manner of mounting can affect the directivity pattern. Thus, the directivity of cooling fan noise shall be worked out by measuring and analysing the spatial distribution of its sound field. One such example is obtained: the directivity data reported by Czolbe and Hecht

[46], in which cooling fan noise dominates can be as approximated by

$$\Delta L_{\mathrm{H}}^{T}(\varphi) = 10\lg[0.25 + 0.75\cos(\varphi)]. \tag{26}$$

Since for various traction units, a wide spread in sound power can be expected; directivity data for each type of traction unit may need to be collected and analysed. However, probably, the directivity of traction noise is in general not important, especially when integrated pass-by noise is concerned. For example, the directivity given by Eq. (26) will have the effect of $-[0.5\ 1.1\ 2.0]$ dB at respective angle positions of $[30\ 45\ 60]^{\circ}$.

The directivity of impact sound should be the same as that of rolling noise. Braking at speed will produce broadband noise [48]; thus, the directivity of it should be the same as that of the wheel radiation. Braking at very low speed will frequently induce brake squeal noise. Brake squeal noise and curve squeal noise may be of the same directivity character as that of wheel radiation, while carefulness should be paid, because the directivity of wheel radiation has been determined based on the data in one-third octave bands and for wheels with a curved web. It is not sure if this directivity is also valid for a vibrating wheel with a straight web excited at a narrow frequency. To answer this question, further measurement investigation is required.

There are two main reasons for noise amplification by a bridge: (1) because of its large radiation surface, a bridge acts as a *sounding board*; (2) the rail itself may vibrate considerably greater than for track at grade [10]. Since a sounding board is likely less directional than a vibrating rail, the directivity of bridge noise differs from, while is likely less directional than, that of the rail radiation. Presently, no such directivity data have been reported.

5. Concluding remarks and some further discussion

In this article, the directivity of railway noise has been studied extensively and systematically, based on available measurement data and relevant theoretical investigations. A model of *perpendicular dipole pair* is proposed to understand the directivity of wheel/rail vibration noise and the directivity of the pantograph noise. For aerodynamic noise around bogies *scattering* of the air flow is proposed to be the dominant mechanism of the noise generation. Discussions are made in a systematic way and all the (available) directivity measurements are reflected. The directivity functions, or, the calculation procedures to construct directivity functions have been proposed for the dominant noise types. Since many different situations have been discussed, for the convenience of potential readers, all equations appeared in this article are summarized in Table 2 together with respective conditions.

It is found that the model of *perpendicular dipole pair* can properly explain the measurement specified directivity characteristics of wheel/rail vibration noise and pantograph noise. And, unintentionally, turbulent boundary layer noise and scattered fluid sound also form a perpendicular dipole pair, although the latter predominates in sound power. Moreover, based on this understanding, the former proposal for the directivity of aerodynamic noise [17], given by Eq. (15) in this paper, is found not to be suitable for aerodynamic noise around bogies. The directivity given by Eq. (24) seems a

Table 2
Equations and respective conditions.

Eqs.	Function	Condition/note
(1)	Directivity of wheel vibration noise	Railway wheels with a curved web; not sure if applicable also for wheels with a straight web
(2)	Horizontal directivity of rolling noise	Rail radiation is assumed 3 dB 'stronger than wheels'. See also Eq. (4)
(3), (3′)	To construct horizontal directivity of rolling noise	Transfer functions must be known when using Eq. (3)
(4)	Horizontal directivity of rolling noise	Wheel radiation is assumed 1 dB stronger than rail's. See also Eq. (2)
(5)	Vertical directivity of rail vibration noise	Rail radiation only
(6)	Vertical directivity of rolling noise	Including shielding effect of rectangular-shape wagons
(7)–(9)	Modelling the vertical directivity of rail vibration noise given by Eq. (5)	Perpendicular dipole pair with vertical component 4 dB weaker
(10)–(12)	A roughness-transfer function expression of wheel noise, rail noise and the combined rolling noise	Roughness, transfer function, wagon length and number of axles per wagon must be known
(13)	The Doppler factor of multipoles	Named as *motion term* in this paper
(14)	Horizontal directivity of rolling noise, including the Doppler factor	The *source term* is given by Eq. (3)
(15)	The Harmonoise proposal for the horizontal directivity of aero-noise	Not for pantograph noise. Eq. (15) is equivalent to Eq. (19)
(16)–(18)	Horizontal directivity of pantograph noise	The directivity data were given in [17]
(19)–(21)	Horizontal directivity of turbulent boundary layer noise	Based on Tam's work [41]
(22)	Scattered fluid sound by a compact, rigid and fixed sphere	Rayleigh scattering and plane wave
(23)	Scattered fluid sound by a rough wall	Rayleigh scattering; $\omega R/v_* > 5$
(24)	Horizontal directivity of combined scattered fluid sound and turbulent boundary layer noise	C_1=0.1 or b=0.01 if 10 or 20 dB difference in components' sound power
(25)	Combined horizontal directivity of scattered fluid sound	At 350 km/h; source term is given by Eq. (24)
(26)	Horizontal directivity of the locomotive cooling fan noise	Based on the directivity data given in [46]

proper one for this noise component. Furthermore, this directivity character also suggests a possibility to separate aerodynamic noise around bogies from the rolling noise.

Vertical directivity of wheel/rail vibration noise is given by Eq. (5), or equivalently by Eq. (1), because the difference between these two functions is not important. However, in practice, there are many factors, which can significantly affect the equivalent vertical directivity. Those factors can be the shielding of the car body, the shielding and/or reflection and/or diffraction of near-track objects such as low barriers or viaduct banks, radiation from vibrating foundations such as a vibrating viaduct or bridge, ground reflection and absorption. Therefore, vertical directivity shall in general be determined for each train type and even at each location if concerned terrains are much different; no universal description for vertical directivity can be expected. Nevertheless, this quantity has to be handled in railway noise engineering, because it is an important parameter for evaluating noise impact from rail vehicles on near-line high rise buildings. What could be improved in future would be a description of the vertical directivity for categorised situations, based on extensive measurement investigations.

Without considering high speed trains, i.e. with rolling noise dominates, "the detailed directivity is of little practical relevance. It is sufficient to obtain an indication of the approximate nature of the directivity" [35]. This conclusion is acceptable for those applications which concern conventional speeds. For example, according to Eq. (2) which gives the horizontal directivity of the rolling noise, the directivity effects are - [1.0 2.4 4.4] dB for angle positions of [30 45 60]°, respectively. Since the peak radiation is in the lateral normal direction, using the accurate horizontal directivity of rolling noise compared with simply using dipole directivity makes no important correction on pass-by rolling noise. This fact explains why people can talk about 2 dB accuracy even without proper description of horizontal directivity for the noise sources. However, this is no longer the case for high speed trains, where aerodynamic noise becomes comparable to or more important than the rolling noise. As has been indicated by this study, peak radiation of scattered fluid sound around bogies is in the direction of motion. Therefore, a proper description of its horizontal directivity is important to determine the total wayside radiation of aerodynamic noise during a train pass-by.

Discussions on the directivities of other noise types, except traction noise are mainly in principle and qualitatively, due to the reasons of that these noise types are related to the wheel/rail vibration noise and that no such directivity data are available presently. These discussions, although they serve as a complement part to complete the survey of the directivities of important railway noise sources, are not intended for replacing necessary further measurement investigation on the directivities.

The dipole directivity function, $D_{\text{dipole}} = 10\lg[0.01 + 0.99\cos^2(\varphi)]$, was adopted by the European IMAGINE project [49] for the horizontal directivity of the rolling noise. As has been discussed in this paper, (1) wheel radiation is not a dipole source and (2) its importance relative to the rail radiation increases with train speed. The horizontal directivity of rolling noise at about 150 km/h is given by Eq. (2) and that at about 350 km/h is likely given by Eq. (4). These three directivity functions at horizontal angles (to the track normal) of [20° 40° 60° 80°] (degrees) are compared in Table 3.

For aerodynamic noise around bogies, the directivity functions given by Eq. (15) and (24) are compared in Table 4.

To validate if Eq. (24) correctly describes the horizontal directivity of the aerodynamic noise around bogies (or, equivalently, if scattering is the dominant mechanism for the noise generation), some particular measurements can be considered. The key point is to separate pantograph noise from other important noise components (rolling noise and aerodynamic noise around bogies). And, it will be equivalent if pantograph noise can accurately be measured in a separate way. When pantograph noise can be handled, one can consider to measure the bogie noise of a passing-by train at angle positions of [10° 30° 50° 70° 90° 110° 130° 150° 170°] degrees to the track with a measurement radius about twice the train length (then, a short train is preferred), by using, probably, Ultimate Sound Probes (USPs) [50]. The train speed is better not

Table 3
The comparison of the three horizontal directivity functions proposed for railway rolling noise (the digits are the differences to a monopole source).

Directivity (dB)	Horizontal angle to the track normal (degrees)			
	20°	40°	60°	80°
$D_{\text{dipole}} = 10\lg[0.01 + 0.99\cos^2(\varphi)]$	−0.53	−2.88	−5.89	−14.00
$10\lg[0.15 + 0.85\cos^2(\varphi)]$	−0.45	−1.88	−4.41	−7.55
$10\lg[0.23 + 0.35\cos(\varphi) + 0.42\cos^2(\varphi)]$	−0.32	−1.28	−2.92	−5.18

Table 4
The comparison of the two horizontal directivity functions proposed for railway aerodynamic noise (the digits are the differences to a monopole source).

Directivity (dB)	Horizontal angle to the track normal (degrees)			
	20°	40°	60°	80°
$5\ln[\sin(\varphi + \pi/2)]$	−0.31	−1.33	−3.47	−8.75
$10\lg[0.03 + 0.97\cos^2(\varphi - \pi/2)]$	−8.43	−3.66	−1.21	−0.13

less than 350 km/h, in order to guarantee the importance of aerodynamic noise relative to the rolling noise. For the aerodynamic noise components, the effect of the Doppler factor will be corrected using Eq. (25). The terrain of a measurement site should be reasonably uniform and meteorological conditions should have negligible influence on the horizontal directivity of train pass-by noise. Since the rolling noise can be evaluated using the TWINS model provided all the input parameters are available, the horizontal spatial distribution of the aerodynamic sound around bogies can then, in principle, be obtained.

Moreover scattered fluid sound around bogies is of dipole directivity with the dipole axis being parallel to the track. Then, in the vertical plane perpendicular to the track, it shall present the directivity of monopole feature. Therefore, if it would become a predominant source, the train pass-by noise would be ψ—independent, where ψ is the vertical angle in y–z plane as defined in Fig. 1.

As for the pantograph noise, in the vertical plane containing the track central line and at a position high above the track, pantograph noise should present dipole directivity based on the discussion in Section 3.1.2. The difficulty to validate this understanding is that there is no effective method to separate pantograph noise from the other important noise components, of which vertical directivities, in this vertical plane, are still an unsolved problem.

Acknowledgement

The author is grateful to the referees for their constructive comments on the manuscript. Dr. Hans Jonasson reads the revised manuscript and provides his detailed comments on the revision.

References

[1] Wolfgang Kropp, Tor Kihlman, Jens Forssén and Lars Ivarsson, Reduction potential of road traffic noise—a pilot study, The Department of Applied Acoustics, Chalmers University of Technology, February 2007.
[2] European Environment Agency, TERM 2001, Indicators tracking transport and environment integration in the European Union, Copenhagen, 2001.
[3] WG Railway Noise of the European Commission, Position paper on the European strategies and priorities for railway noise abatement, 2003.
[4] Paul J. Remington, Wheel/rail noise, I: characterization of the wheel/rail dynamic system, *Journal of Sound and Vibration* 46 (1976) 359–379.
[5] M.J. Rudo, Wheel/rail noise—part II: wheel squeal, *Journal of Sound and Vibration* 46 (1976) 381–394.
[6] I.L. Vér, C.S. Ventres, M.M. Myles, Wheel/rail noise—part III: impact noise generation by wheel and rail discontinuities, *Journal of Sound and Vibration* 46 (1976) 395–417.
[7] Paul J. Remington, Wheel/rail noise—part IV: rolling noise, *Journal of Sound and Vibration* 46 (1976) 419–436.
[8] A.G. Galaitsis, E.K. Bender, Wheel/rail noise—part V: measurement of wheel and rail roughness, *Journal of Sound and Vibration* 46 (1976) 437–451.
[9] D.J. Thompson, Wheel–rail noise: theoretical modelling of the generation of vibration, Ph.D. thesis, University of Southampton (1990).
[10] David Thompson, in: *Railway Noise and Vibration: Mechanisms, Modelling and Means of Control*, Elsevier, 2009.
[11] Final International Seminar, The results of the Dutch Noise Innovation Programme—Railways (IPG-Rail), Doorn, The Netherlands, 9 December, 2008.
[12] W. Behr, T. Lölgen, W. Baldauf, L. Willenbrink, R. Blaschko, K. Jäger and J. Kremlacek, Low noise pantograph ASP—recent developments, in: *Proceedings of the Inter Noise 2000*, Nice (France), 27–30 August, 2479–2484.
[13] C. Noger, J.C. Patrat, J. Peube, J.L. Peube, Aerodynamical study of the TGV pantograph recess, *Journal of Sound and Vibration* 231 (2000) 563–575.
[14] T. Okamura, Y. Kusumi, T. Hariyama, Development and prospect for low noise pantographs, in: *Proceedings of the Inter Noise 2000*, Nice (France), 27–30 August, 2468–2473.
[15] H. Matsumoto, K. Saitoh and T. Issiki, A method of reducing aerodynamic sounds generated by bent round bars in a uniform air-flow, in: *Proceedings of the Inter Noise 2006*, Honolulu, Hawaii (USA), 3–6 December.
[16] C. Mellet, F. Létourneaux, F. Poisson, C. Tallote, High speed train noise emission: latest investigation of the aerodynamic/rolling noise contribution, *Journal of Sound and Vibration* 293 (2006) 986–994.
[17] C. Charbonnel, Definition of a simple model of sources for the TGV-R, *HAR12TR-021206-SNCF01* (the Harmonoise technical report).
[18] F. Poisson, P.E. Gautier and F. Letourneaux, Noise Sources for High Speed Trains: a Review of Results in the TGV Case, Noise and Vibration Mitigation for Rail Transportation Systems, *Notes on Numerical Fluid Mechanics and Multidisciplinary Design*, Volume 99, ©2008 Springer-Verlag, Berlin Heidelberg.
[19] W.F. King III, A précis of developments in the aeroacoustics of fast trains, *Journal of Sound and Vibration* 193 (1996) 349–358.
[20] C. Talotte, P.E. Gautuer, D.J. Thompson, C. Hanson, Identification, modeling and reduction potential of railway noise sources: a critical survey, *Journal of Sound and Vibration* 267 (2003) 447–468.
[21] B.S. Holmes, J.B. Dias, B.A. jaroux, T. Sassa, Y. Ban, Predicting the wind noise from the pantograph cover of a train, *International Journal for Numerical Methods in Fluids* 24 (1997) 1307–1319.
[22] T. Sassa, T. Sato, S. Yatsui, Numerical analysis of aerodynamic noise radiation from a high-speed train surface, *Journal of Sound and Vibration* 247 (2001) 407–416.
[23] X. Gloerfelt, C. Bailly, D. Juvé, Direct computation of the noise radiated by a subsonic cavity flow and application of integral methods, *Journal of Sound and Vibration* 266 (2003) 119–146.
[24] F. Mizushima, C. Kato, T. Kurita and A. Lida, Investigation of aerodynamic noise generated from a train car gap, in: *Proceedings of the Inter Noise 2006*, Honolulu, Hawaii (USA), 3–6 December.
[25] S. Peters, The prediction of railway noise profiles, *Journal of Sound and Vibration* 32 (1974) 87–99.
[26] X. Zhang, Measurements of directivity on test rig, *HAR12TR-020910-SP04*, 30 April, 2003 (the Harmonoise technical report).
[27] X. Zhang, H. Jonasson, Directivity of railway noise sources, *Journal of Sound and Vibration* 293 (2006) 995–1006.
[28] Xuetao Zhang, To determine the horizontal directivity of a train pass-by, in03_627, in: *Proceedings of the Inter Noise 2003*, Jeju (Korea), 25–28 August.
[29] X. Zhang, Directivity of Railway Rolling Noise, Noise and Vibration Mitigation for Rail Transportation Systems, *Notes on Numerical Fluid Mechanics and Multidisciplinary Design*, Volume 99, ©2008 Springer-Verlag, Berlin, Heidelberg.
[30] C.H. Chew, Vertical directivity of train noise, *Applied Acoustics* 51 (2) (1997) 157–168.
[31] C.H. Chew, Vertical directivity pattern of train noise, *Applied Acoustics* 55 (3) (1998) 243–250.
[32] W.K. Lui, K.M. Li, C.W.M. Leung, G.M. Frommer, An experimental study of the vertical directivity pattern of wheel/rail rolling noise, *Acta Acustica united with Acustica* 93 (2007) 742–749.
[33] T. Ten Wolde, C.J.M. van Ruiten, Sources and mechanisms of wheel/rail noise: state-of-art and recent research, *Journal of Sound and Vibration* 87 (1983) 147–160.

[34] D.J. Thompson, C.J.C. Jones, Sound radiation from a vibrating railway wheel, *Journal of Sound and Vibration* 253 (2002) 401–419.
[35] D.J. Thompson, C.J.C. Jones, N. Turner, Investigation into the validity of two-dimensional models for sound radiation from waves in rails, *Journal of Acoustical Society of America* 113 (2003) 1965–1974.
[36] T. Kitagawa, D.J. Thompson, The horizontal directivity of noise radiated by a rail and implications for the use of microphone arrays, *Journal of Sound and Vibration* 329 (2010) 202–220.
[37] J.J.A. van Leeuwen, M.A. Ouwerkerk, *Comparison of some prediction models for railway noise used in Europe*, Report L.94.0387.A, DGMR consulting engineers bv, The Hague, The Netherlands, (1997).
[38] M.S. Howe, in: *Theory of Vortex Sound*, Cambridge University Press, 2003.
[39] M.H.A. Janssens, M.G. Dittrich, F.G. de Beer, C.J.C. Jones, Railway noise measurement method for pass-by noise, total effective roughness, transfer functions and track special decay, *Journal of Sound and Vibration* 293 (2006) 1007–1028.
[40] M.S. Howe, in: *Acoustics of Fluid–Structure Interactions*, Cambridge University Press, 1998.
[41] K.W. Christopher, Tam, Intensity, spectrum, and directivity of turbulent boundary layer noise, *Journal of Acoustical Society of America* 57 (1975) 25–34.
[42] Lucio Maestrello, Measurement and analysis of the response field of turbulent boundary layer excited panels, *Journal of Sound and Vibration* 2 (1965) 270–292.
[43] Lucio Maestrello, Use of turbulent model to calculate the vibration and radiation responses of a panel, with practical suggestions for reducing sound level, *Journal of Sound and Vibration* 5 (1967) 407–448.
[44] Transportation Paul Nelson, *Noise, Reference Book*, Butterworth & Co. Ltd., 1987.
[45] X. Zhang, Railway traction noise—the state of the art, *HAR12TR-030530-SP01* (the Harmonoise technical report).
[46] C. Czolbe and M. Hecht, Noise reduction measures at freight train locomotives "Blue Tiger", Noise and Vibration Mitigation for Rail Transportation Systems, *Notes on Numerical Fluid Mechanics and Multidisciplinary Design*, Volume 99, ©2008 Springer-Verlag Berlin Heidelberg.
[47] S. Glegg, Fan noise, chapter 19, noise and vibration, in: R.G. White, J.G. Walker (Eds.), Ellis Horwood Ltd., 1982.
[48] M. Dittrich, The IMAGINE source model for railway noise prediction, *Acta Acustica United with Acustica* 93 (2007) 185–200.
[49] 〈www.imagine-project.org〉.
[50] 〈http://www.microflown.com/〉.